nature chemistry

ARTICLES

PUBLISHED ONLINE: 15 MARCH 2009 | DOI: 10.1038/NCHEM.120

Imaging intracellular viscosity of a single cell during photoinduced cell death

Marina K. Kuimova[1,2]*, Stanley W. Botchway[3], Anthony W. Parker[3], Milan Balaz[4], Hazel A. Collins[4], Harry L. Anderson[4], Klaus Suhling[5] and Peter R. Ogilby[2]*

Diffusion-mediated cellular processes, such as metabolism, signalling and transport, depend on the hydrodynamic properties of the intracellular matrix. Photodynamic therapy, used in the treatment of cancer, relies on the generation of short-lived cytotoxic agents within a cell on irradiation of a drug. The efficacy of this treatment depends on the viscosity of the medium through which the cytotoxic agent must diffuse. Here, spectrally resolved fluorescence measurements of a porphyrin-dimer-based molecular rotor are used to quantify intracellular viscosity changes in single cells. We show that there is a dramatic increase in the viscosity of the immediate environment of the rotor on photoinduced cell death. The effect of this viscosity increase is observed directly in the diffusion-dependent kinetics of the photosensitized formation and decay of a key cytotoxic agent, singlet molecular oxygen. Using these tools, we provide insight into the dynamics of diffusion in cells, which is pertinent to drug delivery, cell signalling and intracellular mass transport.

Diffusion-mediated cellular processes depend on the hydrodynamic properties of the intracellular matrix. The translational diffusion coefficient D for a given intracellular solute depends on the fluid-phase viscosity of the cytoplasm, as well as on collisions and interactions that occur between the solute and intrinsic cellular macromolecules[1]. Values of D for both small solutes[1–5] and macromolecules[6,7] in mammalian cells can be 5–50 times smaller than those in pure water. Measurements in cell vesicles[8] demonstrated that the local microviscosity can be as high as 140 cP, whereas the microviscosity in the aqueous phase of the cellular cytoplasm is 1–2 centipoise, similar to that of pure water[9–11]. Such large viscosity variations within a cell can influence diffusion and bimolecular reaction rates[12], and must be considered, for example, when developing strategies for drug delivery and cancer therapy.

Fluorescent molecular rotors, in which the non-radiative decay of an excited state can be altered by the ambient viscosity, have emerged as a new modality for measuring the microviscosity in a biological environment[8,13,14]. This approach complements viscosity-dependent fluorescence depolarization work, pioneered by Perrin[15] and Weber[16]. Precise calibration of the rotor response to viscosity can be achieved by using either fluorescence lifetime-based measurements[8] or a ratiometric approach[14]. The present work uses a new type of rotor, constructed as a conjugated porphyrin dimer (**1**, Fig. 1a). The remarkable nonlinear optical properties of **1**, together with its high intracellular uptake, photostability and favourable photophysical properties, have been used to create an efficient photosensitizer for one-photon and two-photon excited photodynamic therapy (PDT) of cancer[17–20]. In PDT, cell death and tissue eradication are achieved on irradiation of the photosensitizer and the subsequent production of cytotoxic species, in particular singlet molecular oxygen, $O_2(a^1\Delta_g)$ (Fig. 1b)[21]. Now, by using the properties of the dimer **1** as both a PDT photosensitizer and a fluorescent ratiometric molecular rotor, we (i) initiate cell death via irradiation of **1** and (ii) monitor changes in the intracellular viscosity of light-perturbed single cells. Finally, we illustrate the effect of the light-induced viscosity change on intracellular diffusion and reaction rates by direct time-resolved single-cell spectroscopic studies of $O_2(a^1\Delta_g)$, monitoring its formation and decay rates with subcellular resolution.

Results

The spectroscopic properties of a butadiyne-linked porphyrin dimer, structurally related to **1**, have been described in terms of two conformations: planar and twisted, referring to the relative position of the porphyrin units[22]. Each conformer is characterized by distinctive absorption and emission spectra. The emission of the dimer in fluid solution is dominated by the lower-energy planar conformation, whereas the emission of the less-stable twisted conformer can be observed in glassy matrices, in which rotation of the two porphyrin units relative to each other is restricted.

The absorption and emission spectra for **1** in solutions of varying viscosity, ranging from 0.6 to 950 cP, are shown in Figs 1c and 2a. The spectral changes that occur with an increase in viscosity are consistent with the formation of increasing amounts of the twisted conformer of **1** (ref. 22) as torsional rotation about the butadiyne link becomes slower in viscous media. Thus, we assign the emission maximum of **1** at 710 nm to the twisted conformation and the emission maximum at 780 nm to the planar conformation.

The calibration, using a ratiometric approach, of the viscosity-dependent rotor response of **1** following 473-nm excitation is shown in Fig. 2a (inset). The plot of the intensity ratio of the two fluorescence peaks of **1** against viscosity in double logarithmic coordinates shows a good linear correlation, as expected from theory[23].

The dimer **1** is efficiently incorporated into live cells[19]. The fluorescence spectrum of **1** in a cell (Fig. 2b) clearly shows two well-resolved maxima at approximately 710 and 780 nm, corresponding to emission from the twisted and planar conformations of the dimer, respectively. Using the viscosity calibration graph (Fig. 2a, inset), we ascertain that the viscosity of the intracellular

[1]Chemistry Department, Imperial College London, Exhibition Road, London SW7 2AZ, UK, [2]Center for Oxygen Microscopy and Imaging (COMI), Department of Chemistry, University of Aarhus, Århus DK-8000, Denmark, [3]Central Laser Facility, Science and Technology Facilities Council, Rutherford Appleton Laboratory, Harwell Science and Innovation Campus, Didcot, Oxfordshire OX11 0QX, UK, [4]Oxford University, Department of Chemistry, Chemistry Research Laboratory, Oxford OX1 3TA, UK, [5]Department of Physics, King's College London, Strand, London WC2R 2LS, UK.
*e-mail: m.kuimova@imperial.ac.uk; progilby@chem.au.dk

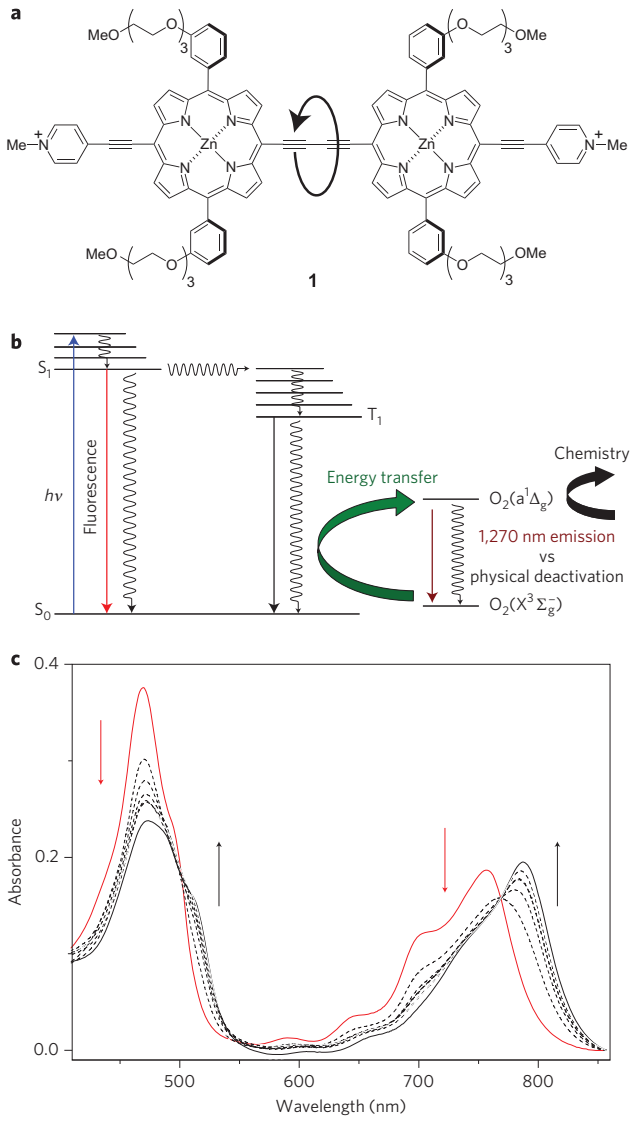

Figure 1 | Principles of intracellular viscosity detection and singlet-oxygen generation using a porphyrin dimer. a, Structure of the porphyrin-dimer-based rotor **1**. **b**, Schematic representation of one-photon photosensitized singlet-oxygen production: irradiation of the sensitizer (for example **1**) populates a singlet excited state, S_1; intersystem crossing from S_1 produces a long-lived triplet state, T_1; energy transfer from T_1 to ground-state oxygen, $O_2(X^3\Sigma_g^-)$, generates singlet oxygen, $O_2(a^1\Delta_g)$. **c**, Absorption spectra of **1** in methanol/glycerol mixtures of increasing viscosity, from 0.6 cP (methanol, red line) to 950 cP (95% glycerol, solid black line). The changes in absorption are consistent with the formation of increasing amounts of the twisted conformer of **1** in more-viscous media. Arrows indicate the direction of change on irradiation.

compartments where **1** localizes is approximately 50 cP (see Supplementary Information). A similarly high viscosity has been reported for endocytotic vesicles of live cells[8].

The fluorescence spectrum of **1** was also recorded in the bulk cell culture medium (Fig. 2b). Here, the emission spectral shape shows only a slight deviation from that in non-viscous solutions (Fig. 2a). The small increase in apparent viscosity measured by **1** in the culture medium compared with methanol corresponds to the surface binding of **1** to bovine serum albumin (BSA), as previously established for a series of ionic dimers similar to **1** (ref. 19) and for smaller charged porphyrins[24,25]. As the dimer **1** is too large for highly specific 'lock–key' binding with intracellular proteins[26] that, in turn, would restrict its conformational dynamics, the spectrum of intracellular **1** must reflect a large ambient viscosity rather than specific binding. This point is corroborated by independent singlet-oxygen experiments (see below).

An important advantage of monitoring intracellular microviscosity using molecular rotors is the possibility of characterizing a dynamically changing environment. We illustrate this by recording emission spectra of **1** inside cells during PDT; that is, on irradiation with light, which ultimately results in cell death (Fig. 2c).

On irradiation with light, **1** sensitizes the production of cytotoxic $O_2(a^1\Delta_g)$ (ref. 19; Fig. 1b) and initiates cell death[17,20]. The series of emission spectra obtained on irradiation of **1** in a single cell (Fig. 2c) correspond to a significant increase in the viscosity of the intracellular environment surrounding **1**. Importantly, the spectrum obtained for **1** in a cell-culture medium does not change shape on 473-nm irradiation (Fig. 2c, inset), suggesting that the behaviour observed for **1** in a cell is not a result of binding to proteins. Using the calibration graph (Fig. 2a, inset), we determined the post-PDT viscosity of the cellular domains containing **1** as 300 ± 50 cP. This value is significantly greater than that obtained before PDT (see above). This viscosity increase probably reflects crosslinking reactions, mediated by singlet oxygen or secondary reactive radicals, similar to those observed in model and intracellular protein systems[27–30].

Increased viscosity can alter the rate of many diffusion-dependent processes in a cell. We set out to establish the effect of the photoinduced change in intracellular viscosity on the kinetics of photosensitized formation and decay of cytotoxic $O_2(a^1\Delta_g)$. It has been demonstrated that, in spite of the extremely low quantum yield of its emission (of the order of 10^{-6}), $O_2(a^1\Delta_g)$ can be monitored by its 1,270 nm phosphorescence in single cells[31,32]. Figure 3a shows averaged $O_2(a^1\Delta_g)$ phosphorescence traces recorded at 1,270 nm after excitation of **1** in cells. The two traces were obtained from the same cell location on initial and prolonged irradiation. The observed irradiation-dependent decrease in the rate of signal decay, from $(16 \pm 2\ \mu s)^{-1}$ to $(28 \pm 3\ \mu s)^{-1}$, suggests an increase in the viscosity of the environment in which $O_2(a^1\Delta_g)$ has been produced, with a corresponding decrease in the rate of bimolecular quenching[12] (see Supplementary Information).

5,10,15,20-Tetrakis(*N*-methyl-4-pyridyl)-21*H*,23*H*-porphine (TMPyP, **2**, Fig. 3b) is a well-studied $O_2(a^1\Delta_g)$ sensitizer[12,31,32]. We now turn to the use of TMPyP to investigate the effect of irradiation-induced viscosity changes on $O_2(a^1\Delta_g)$ kinetics. The 1,270 nm $O_2(a^1\Delta_g)$ traces recorded as a function of elapsed irradiation time of intracellular TMPyP are shown in Fig. 3b. The data clearly show irradiation-dependent decreases both in the rate of signal decay, from $(23.7 \pm 0.8\ \mu s)^{-1}$ to $(30 \pm 1\ \mu s)^{-1}$, and in the rate of signal formation, from $(\ll 1\ \mu s)^{-1}$ to $(6 \pm 1\ \mu s)^{-1}$. These changes are consistent with an increase in viscosity that influences bimolecular events that result in (i) $O_2(a^1\Delta_g)$ formation, that is, triplet-state sensitizer deactivation by oxygen, and (ii) $O_2(a^1\Delta_g)$ decay, that is, collisions with intracellular quenchers.

These irradiation-induced changes in the $O_2(a^1\Delta_g)$ phosphorescence signals occur on approximately the same timescale of elapsed irradiation as the fluorescence spectral change of the molecular rotor (Fig. 2c, inset). The coincidence of these timescales, and the fact that we observe a change in both the triplet deactivation rate and singlet oxygen lifetime, allows us to rule out the depletion of oxygen in the local environment of the photosensitizer as a reason for the observed changes in the time-resolved 1,270 nm signals. In fact, the integrated intensity of the $O_2(a^1\Delta_g)$ phosphorescence signal increases as irradiation time elapses, suggesting an increase, not a decrease, in the local oxygen concentration. The latter would be observed if $O_2(a^1\Delta_g)$ were produced in hydrocarbon-dominated domains where the solubility of oxygen is much higher than in an aqueous phase[33], which is consistent with

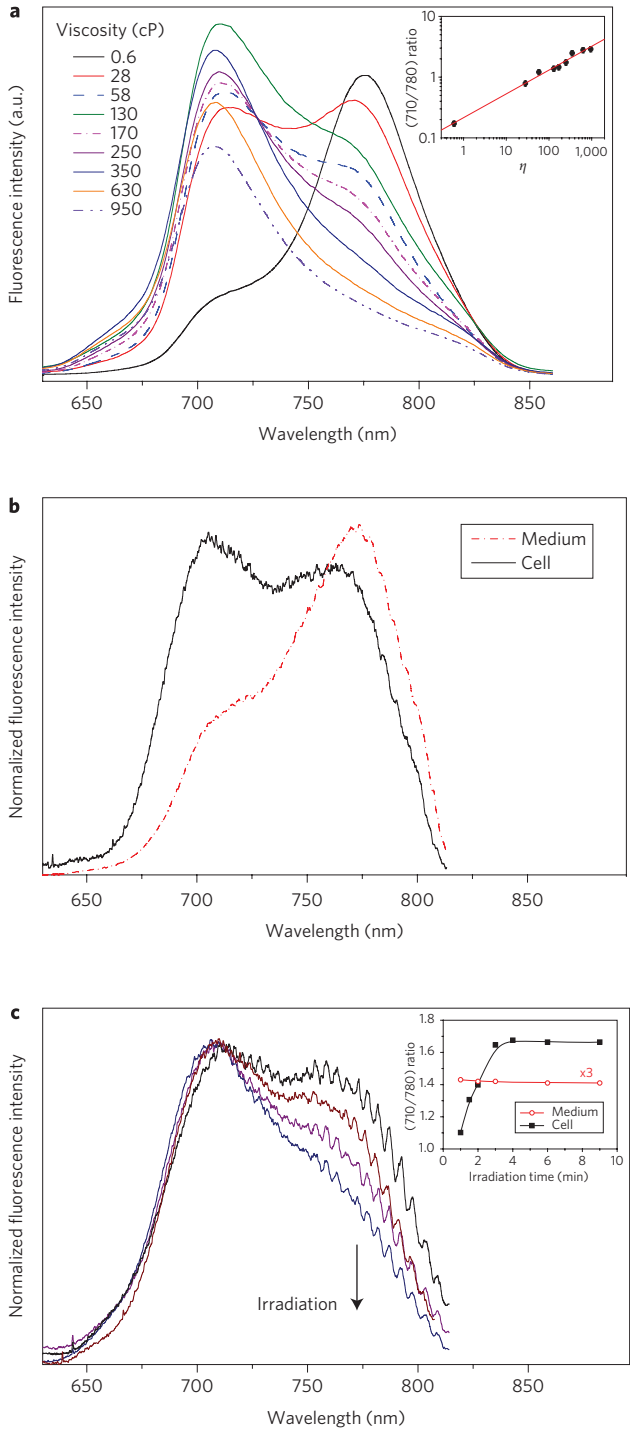

Figure 2 | Emission spectra obtained upon 473 nm excitation of 1 in solution and in cells. a, Excitation in methanol/glycerol mixtures of different viscosities. The inset is a double logarithmic plot of the intensity ratio of the emission peaks at 710 and 780 nm versus solution viscosity. The changes in emission are consistent with the formation of increasing amounts of the twisted conformer of **1** in more-viscous media, and this makes ratiometric viscosity calibration possible. **b**, Excitation in a cell (black) and in the bulk culture medium supplemented with 10% FCS (red). **c**, Excitation in a cell recorded as a function of time following irradiation at 473 nm (0.1 mW, 1 min per spectrum). The arrow indicates the direction of change on irradiation. The inset shows the intensity ratio of the emission peaks at 710 and 780 nm versus irradiation time in a cell (black) and in the culture medium, ×3 (red). The intracellular intensity ratio increases following irradiation, corresponding to a significant increase in local microviscosity.

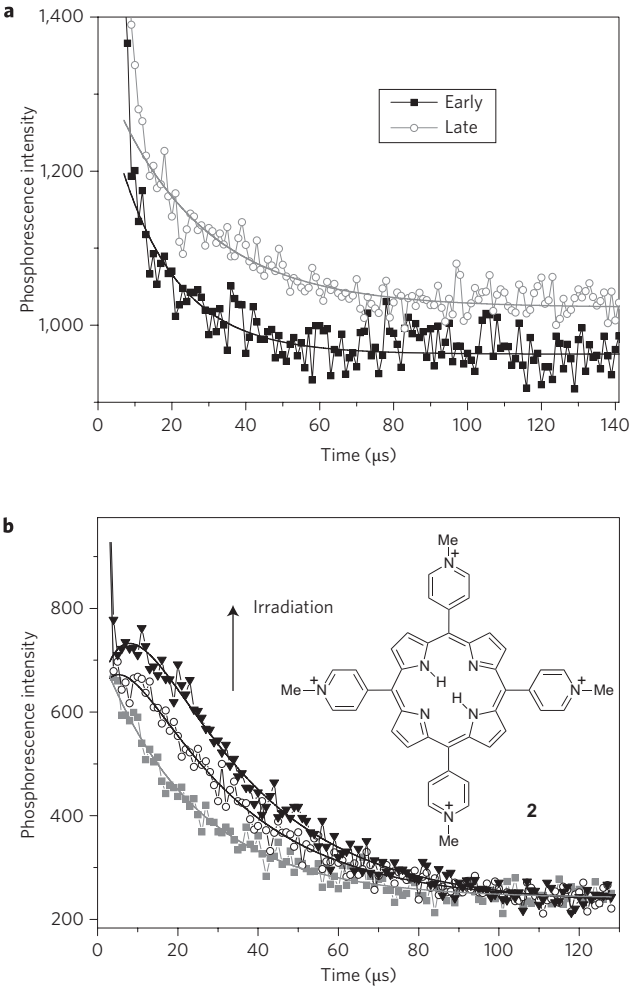

Figure 3 | Time-resolved singlet-oxygen phosphorescence traces recorded at 1270 nm from D_2O-incubated cells. a, Signals produced on 790 nm irradiation of **1** in a cell: black squares, trace obtained in the first 3 min of irradiation; circles, trace obtained from the same cell location in a subsequent 3 min period. Traces are offset for clarity, and each was obtained by averaging measurements from five cells. **b**, Signals produced on 420-nm irradiation of TMPyP (**2**) in a single location of a cell over three subsequent periods of 3-min irradiation. The arrow indicates the direction of change on irradiation.

photoinitiated crosslinking leading to intracellular domains of high viscosity. In short, PDT treatment of cells indeed results in a viscosity-dependent decrease in the diffusion and bimolecular reaction rates of species in a cell.

In the highly heterogeneous environment of a viable cell, it is particularly attractive to be able to obtain a spatially resolved image of intracellular viscosity. Here we use the spectrally resolved fluorescence measurements of **1** to obtain ratiometric viscosity maps of a cell as a function of elapsed irradiation time (Fig. 4). These images clearly show that the intracellular viscosity is inhomogeneous and that intracellular viscosity increases during irradiation.

Discussion

We have reported a new type of ratiometric fluorescent molecular rotor suitable for quantifying and imaging intracellular viscosity in live cells. The rotor enables real-time monitoring of dynamic processes in cells. This has been illustrated by quantifying a significant increase in intracellular viscosity during photoinduced cell death. We have also demonstrated that such a viscosity increase indeed alters diffusion-dependent kinetics in a cell, illustrated through

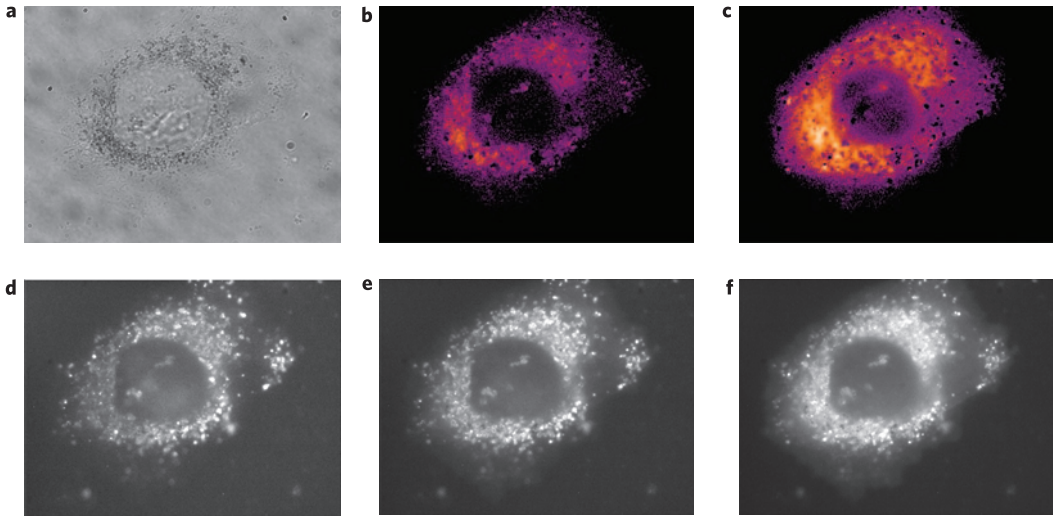

Figure 4 | Imaging changes in intracellular viscosity using 1 in the ratiometric approach. a–c, Transmission image (**a**) and ratiometric fluorescence (**b**,**c**) images of **1** in a cell ($\lambda_{ex} = 480 \pm 15$ nm) obtained during initial (**b**) and advanced (**c**) stages of irradiation; violet corresponds to lower viscosity and orange to higher viscosity, and all viscosities are in the range $\gg 1$ cP. **d–f**, Conventional fluorescence intensity images from which the ratiometric images were obtained using ImageJ software. The intensity image with $\lambda_{det} = 700 \pm 20$ nm (**e**,**f**), recorded in either the initial (**e**) or advanced (**f**) stages of irradiation, was divided by the intensity image with $\lambda_{det} = 800 \pm 20$ nm (**d**). Image (**d**) remained unchanged during irradiation. The changes from (**b**) to (**c**) and from (**e**) to (**f**) demonstrate that the intracellular viscosity increases during irradiation.

changes in the photosensitized production and subsequent decay of the cytotoxic species singlet oxygen, $O_2(a^1\Delta_g)$. A major challenge when studying dynamic biological systems is that one must constantly consider phenomena that alter the heterogeneous submicrometre environment of a cell. In this report, we have presented tools that will help to unravel the underlying mechanisms of such processes.

Methods

The viscosity of the methanol/glycerol mixtures at 22 °C was measured as described previously[8] (see Supplementary Information).

Carcinoma of the Chinese hamster ovary (CHO) and HeLa cell lines were obtained from the European Collection of Cell Cultures (ECACC). Cells were cultured in 10 cm^3 flasks at 37 °C in 5% CO_2 in Dulbecco's modified Eagle's medium (DMEM) with 10% fetal calf serum (FCS), penicillin and streptomycin antibiotics, and were passaged when 70–90% confluent. For fluorescence imaging, cells were seeded at 10^4 cells per well in 0.2 ml of culture medium in untreated 8-well coverglass chambers (Lab-Tek) and allowed to grow to confluence for 24 h. The culture medium was replaced with a culture medium containing 10 μM of **1** or TMPyP and incubated for 20 h. To facilitate incorporation of **1**, the culture medium for incubation was prepared by dilution from 1.0 mM stock of **1** in DMSO. Following incubation, the chambers were washed twice with phosphate-buffered saline (PBS), and images were taken at 22 °C. The CHO cell line was used in all experiments with **1**. The HeLa cell line was used in all experiments with TMPyP. Under our experimental conditions, **1** localizes in the cell cytoplasm[19] and TMPyP localizes in the cell nucleus and the cytoplasm[12,31,32]. On excitation of TMPyP, the fluorescence and singlet-oxygen signals can be detected independently from both cell locations.

Fluorescence cell imaging was performed by irradiating the entire cell and its surroundings with a steady-state Xe lamp, using interference filters to select the appropriate excitation wavelength. Light emitted by the sample was detected through interference filters using a charge-coupled device (CCD) camera (Evolution QEi controlled by ImagePro software, Media Cybernetics) placed at the image plane of the microscope. Bright-field images were recorded using the same CCD camera, and backlighting was achieved with a tungsten lamp provided as an accessory to an Olympus IX70 inverted microscope using an oil-immersion ×100 objective (NA = 1.30). The ratiometric images were obtained using ImageJ software (see Supplementary Information).

The fluorescence spectra of **1** from cells were obtained using 473 nm pulsed excitation from a diode laser (Becker & Hickl, BDL-473-SMC, 10 mW, 20 MHz) coupled to a microscope. The output power was attenuated using neutral-density filters to <0.1 mW. The emission was spectrally dispersed using a spectrograph monochromator (Acton, Spectradrive 275) in the range between 500 and 800 nm, and was detected using a CCD (Andor iDus BU440). The CCD was calibrated using the output of a low-pressure mercury lamp (435, 546, 579 and 706 nm) and a HeNe laser (633 nm).

For detection of singlet oxygen, cells to be studied were contained in an atmosphere-controlled chamber that was mounted onto the translation stage of an inverted microscope. The sensitizer that had been incorporated into the cell was irradiated using the output of a femtosecond laser system through the microscope objective (Olympus, IR coating, ×60, NA = 0.90, irradiated spot size approximately 1 μm diameter). The emitted light was collected using the microscope objective, spectrally isolated using an interference filter (1,270 ± 15 nm), and transmitted to a cooled photomultiplier tube, operated in a photon-counting mode, coupled to a multiscaler (MSA 300, Becker & Hickl; see Supplementary Information). In a typical experiment, excitation energies ranged from 3 to 10 nJ per pulse at a repetition rate of 1 kHz. These experiments were performed using cells exposed to an atmosphere of 100% oxygen, which results in the most-intense $O_2(a^1\Delta_g)$ phosphorescence signal[5,32]. During incubation, the H_2O-based DMEM medium was exchanged with a D_2O-based medium, as previously described[31]. This procedure results in a greater quantum efficiency of singlet-oxygen emission, and has no ill effects on the viability of the cells over the time course of our experiments[31].

Received 8 September 2008; accepted 23 January 2009; published online 15 March 2009

References

1. Kao, H. P., Abney, J. R. & Verkman, A. S. Determinants of the translational mobility of a small solute in cell cytoplasm. *J. Cell Biol.* **120,** 175–184 (1993).
2. Jones, D. P. Effect of mitochondrial clustering in O_2 supply in hepatocytes. *Am. J. Physiol.* **247,** C83–C89 (1984).
3. O'Loughlin, M. A., Whillans, D. W. & Hunt, J. W. A fluorescence approach to testing the diffusion of oxygen into mammalian cells. *Radiat. Res.* **84,** 477–495 (1980).
4. Uchida, K., Matsuyama, K., Tanaka, K. & Doi, K. Diffusion coefficient for O_2 in plasma and mitochondrial membranes of rat cardiomyocytes. *Respir. Physiol.* **90,** 351–362 (1992).
5. Hatz, S., Poulsen, L. & Ogilby, P. R. Time-resolved singlet oxygen phosphorescence measurements from photosensitized experiments in single cells: the effect of oxygen diffusion and oxygen concentration. *Photochem. Photobiol.* **84,** 1284–1290 (2008).
6. Wojcieszyn, J. W., Schlegel, R. A., Wu, E. S. & Jacobson, K. A. Diffusion of injected macromolecules within the cytoplasm of living cells. *Proc. Natl Acad. Sci. USA* **78,** 4407–4410 (1981).
7. Seksek, O., Biwersi, J. & Verkman, A. S. Translational diffusion of macromolecule-sized solutes in cytoplasm and nucleus. *J. Cell Biol.* **138,** 131–142 (1997).
8. Kuimova, M. K., Yahioglu, G., Levitt, J. A. & Suhling, K. Molecular rotor measures viscosity via fluorescence lifetime imaging. *J. Am. Chem. Soc.* **130,** 6672–6673 (2008).
9. Dix, J. A. & Verkman, A. S. Mapping of fluorescence anisotropy in living cells by ratio imaging—Application to cytoplasmic viscosity. *Biophys. J.* **57,** 231–240 (1990).

10. Luby-Phelps, K. *et al.* A novel fluorescence ratiometric method confirms the low solvent viscosity of the cytoplasm. *Biophys. J.* **65,** 236–242 (1993).
11. Suhling, K. *et al.* Time-resolved fluorescence anisotropy imaging applied to live cells. *Opt. Lett.* **29,** 584–586 (2004).
12. Kuimova, M. K., Yahioglu, G. & Ogilby, P. R. Singlet oxygen in a cell: Spatially-dependent lifetimes and quenching rate constants. *J. Am. Chem. Soc.* **131,** 332–340 (2009).
13. Haidekker, M. A. & Theodorakis, E. A. Molecular rotors—Fluorescent biosensors for viscosity and flow. *Org. Biomol. Chem.* **5,** 1669–1678 (2007).
14. Haidekker, M. A., Brady, T. P., Lichlyter, D. & Theodorakis, E. A. A ratiometric fluorescent viscosity sensor. *J. Am. Chem. Soc.* **128,** 398–399 (2006).
15. Perrin, F. La fluorescence des solutions: induction moléculaire. Polarisation et durée d'emission. Photochimie. *Ann. Phys. (Paris)* **12,** 169–275 (1929).
16. Shinitzky, M., Dianoux, A. C., Gitler, C. & Weber, G. Microviscosity and order in the hydrocarbon region of micelles and membranes determined with fluorescent probes. I. Synthetic micelles. *Biochemistry* **10,** 2106–2113 (1971).
17. Collins, H. A. *et al.* Blood vessel closure using photosensitisers engeneered for two-photon excitation. *Nature Photon.* **2,** 420–424 (2008).
18. Balaz, M., Collins, H. A., Dahlstedt, E. & Anderson, H. L. Synthesis of biocompatible conjugated porphyrin dimers for one-photon and two-photon excited photodynamic therapy at NIR wavelengths. *Org. Biomol. Chem.* **7,** 874–888, doi:10.1039/b814789b (2009).
19. Kuimova, M. K. *et al.* Photophysical properties and intracellular imaging of water-soluble porphyrin dimers for two-photon excited photodynamic therapy. *Org. Biomol. Chem.* **7,** 889–896, doi:10.1039/b814791d (2009).
20. Dahlstedt, E. *et al.* One- and two-photon activated phototoxicity of conjugated porphyrin dimers with high two-photon absorption cross-sections. *Org. Biomol. Chem.* **7,** 897–904, doi:10.1039/b814792b (2009).
21. Bonnett, R. *Chemical Aspects of Photodynamic Therapy* (Gordon and Breach, 2000).
22. Winters, M. U. *et al.* Photophysics of a butadiyne-linked porphyrin dimer: Influence of conformational flexibility in the ground and first singlet excited state. *J. Phys. Chem. C* **111,** 7192–7199 (2007).
23. Förster, T. & Hoffmann, G. Viscosity dependence of fluorescent quantum yields of some dye systems. *Z. Phys. Chem.* **75,** 63–76 (1971).
24. Borissevitch, I. E., Tominaga, T. T. & Schmitt, C. C. Photophysical studies on the interaction of two water-soluble porphyrins with bovine serum albumin. Effects upon the porphyrin triplet state characteristics. *J. Photochem. Photobiol. A* **114,** 201–207 (1998).
25. Lang, K., Mosinger, J. & Wagnerova, D. M. Photophysical properties of porphyrinoid sensitizers non-covalently bound to host molecules; models for photodynamic therapy. *Coord. Chem. Rev.* **248,** 321–350 (2004).
26. Zunszain, P. A., Ghuman, J., Komatsu, T., Tsuchida, E. & Curry, S. Crystal structural analysis of human serum albumin complexed with hemin and fatty acid. *BMC Struct. Biol.* **3**: 6 (2003).
27. Goosey, J. D., Zigler, J. S. & Kinoshita, J. H. Cross-linking of lens crystallins in a photodynamic system—A process mediated by singlet oxygen. *Science* **208**, 1278–1280 (1980).
28. Dubbelman, T., Degoeij, A. & Vansteveninck, J. Photodynamic effects of protoporphyrin on human erythrocytes—A nature of cross-linking of membrane proteins. *Biochim. Biophys. Acta* **511,** 141–151 (1978).
29. Verweij, H., Dubbelman, T. & Vansteveninck, J. Photodynamic protein cross-linking. *Biochim. Biophys. Acta* **647,** 87–94 (1981).
30. Basu, S., Rodionov, V., Terasaki, M. & Campagnola, P. J. Multiphoton-excited microfabrication in live cells via Rose Bengal cross-linking of cytoplasmic proteins. *Opt. Lett.* **30,** 159–161 (2005).
31. Hatz, S., Lambert, J. D. C. & Ogilby, P. R. Measuring the lifetime of singlet oxygen in a single cell: Addressing the issue of cell viability. *Photochem. Photobiol. Sci.* **6,** 1106–1116 (2007).
32. Snyder, J. W., Skovsen, E., Lambert, J. D. C. & Ogilby, P. R. Subcellular, time-resolved studies of singlet oxygen in single cells. *J. Am. Chem. Soc.* **127,** 14558–14559 (2005).
33. Battino, R. (ed.) *Oxygen and Ozone. Solubility Data Series* **7** (Pergamon, 1981).

Acknowledgements

M.K.K. is grateful to the EPSRC Life Sciences Interface programme for a personal fellowship. We thank STFC for funding access to the Central Laser Facility. This work was supported in part by the Danish National Research Foundation under a block grant for the Center for Oxygen Microscopy and Imaging.

Author contributions

M.K.K. designed the research, M.K.K., S.W.B. and A.W.P. measured fluorescence spectra, M.K.K. performed ratiometric imaging and measured singlet-oxygen traces. M.B. and H.A.C. synthesized the porphyrin dimer. All authors discussed the results and contributed to the manuscript.

Additional information

Supplementary information and chemical compound information accompany this paper at www.nature.com/naturechemistry. Reprints and permission information is available online at http://npg.nature.com/reprintsandpermissions/. Correspondence and requests for materials should be addressed to M.K.K. and P.R.O.